

## Polarization potentials for positron- and electron-atom systems

Hiroshi Nakanishi and D. M. Schrader

*Chemistry Department, Marquette University, Milwaukee, Wisconsin 53233*

(Received 25 November 1985)

Semiempirical polarization potentials with several cutoff functions are investigated for positron- and electron-atom interactions. A disposable parameter, an effective radius, in each cutoff function is adjusted so as to reproduce well-established reference values (scattering lengths and binding energies) in calculations. Striking regularities in fitted parameter values are found despite the very wide variety of cutoff functions examined. The parameter exhibits a strong dependence upon spin and angular momentum in the electronic systems, which is rationalized in terms of the Pauli exclusion principle. Simple semiempirical relations between the effective radii for positronic systems and those for the corresponding electronic systems are proposed, which enable one to find the parameter value for an electron by fitting a positron calculation to a reference value, or vice versa. In other words, the number of adjustable parameters is reduced to a single effective radius for each target regardless of the projectile.

### I. INTRODUCTION

Positron and electron scattering from atoms is one of the simplest and most fundamental problems in atomic physics. It continuously attracts both experimentalists and theorists, and it provides indispensable information on many subjects. Although several *ab initio* calculations have been made for atomic hydrogen and helium and for molecular hydrogen targets, it is practically impossible to solve exactly even low-energy single-channel scattering of  $e^{\pm}$  from atoms much larger than helium. The difficulty arises mainly from polarization effects; that is, distortion or rearrangement of electronic configurations of the target atom by the incident charged particle. If the problem is approached from the point of view of polarization potentials, a consideration of higher excited states is required. To describe this nonlocal polarization potential, several functional forms have been derived for hydrogenic atoms in the context of the adiabatic approximation in first-order perturbation theory. The topic has been reviewed by Drachman and Temkin,<sup>1</sup> Callaway,<sup>2</sup> and recently Peach.<sup>3</sup>

Since semiempirical polarization potentials were first used in electron-scattering calculations by Holtsmark<sup>4</sup> and positron-scattering calculations by Massey and Moussa<sup>5</sup> using the Buckingham potential,<sup>6,7</sup> many others have shown that the intricate polarization effects for atoms and molecules can be described fairly adequately by a simple function with a well-known long-range term and a short-range cutoff function. The inclusion of the correct long-range term is essential in scattering problems. The cutoff function, although its importance has been less emphasized, determines the short-range behavior of the polarization effect on which in many occasions the accuracy of calculations entirely depends.

Since the short-range behavior is expected to be different depending on the systems considered, a cutoff function usually contains a parameter to be adjusted so as to reproduce a well-established property in a calculation, or to be estimated from some reasonable relations. For ex-

ample, a parameter in the Buckingham potential has been originally set to be the radius of each subshell<sup>7</sup> and later adjusted to give the correct polarization potential at the origin.<sup>8</sup> A parameter in a very simple cutoff function recently proposed by one of the present authors has been estimated from regularities observed in the relationship between the ionization potential of the target atom and its scattering length.<sup>9</sup>

For positronic scattering, opposite signs in the static potential and the absence of the exchange potential provide an excellent means to evaluate model polarization potentials for electron scattering.<sup>10</sup> It has been noted, however, that the best polarization potential for a positronic system is not necessarily the best for a corresponding electronic system.<sup>11</sup> The influence of a difference of the incident charge has been demonstrated in a variational perturbation calculation.<sup>1</sup> Recently, this difference has been discussed in detail for positron scattering from molecular hydrogen.<sup>12</sup> Another explanation has been given from the difference in the dynamic terms since an electron accelerates in the core region while a positron decelerates.<sup>13</sup>

Since, in our opinion, additional systematic investigations are needed to elucidate the difference between positron and electron interactions with atoms, we have tested 35 trial polarization potentials for two positronic and four electronic systems in many different bound and scattering states are listed in Table I.<sup>14-20</sup> We have found some simple systematic relationships between positronic and electronic potential parameters. This provides a means for calculating cross sections, binding energies, etc., for positronic systems providing the potential parameters for the corresponding electronic systems are known, or vice versa.

### II. MODEL

#### A. Scattering or orbital equations

The Schrödinger equation for the electronic or positronic orbital or scattering wave function  $\phi$  interacting with

hydrogen or helium atom is, in atomic units,

$$\left[-\frac{1}{2}\nabla^2 + qV_s(r) \pm \delta_{q,-1}K + V_p(r) - \varepsilon\right]\phi(\mathbf{r}) = 0, \quad (1)$$

where  $q$  is the charge of the incident particle,  $V_s$  is the static potential,

$$V_s(r) = \frac{Z}{r} - \sum_i J_i(r), \quad (2)$$

and  $J_i$  is the Coulomb potential for the  $i$ th electronic orbital of the isolated target atom having atomic number  $Z$ . The positive sign in front of the Kronecker delta in Eq. (1) is for singlet systems, and the negative sign is for doublet and triplet systems.  $K$  is the exchange operator which is absent for a positronic system,  $V_p$  is the polarization potential, and  $\varepsilon$  is the eigenvalue for the binding-energy calculation or the incident energy for the scattering

calculation.

The wave function  $\phi$  is expanded in terms of spherical harmonics as

$$\phi(\mathbf{r}) = \sum_{l=0}^{\infty} r^{l-1} f_l(r) Y_{lm}(\theta, \varphi). \quad (3)$$

The radial part of the Schrödinger equation (1) for the  $l$ th partial wave function  $f_l$  is then given by

$$\left[-\frac{1}{2} \left[ \frac{d^2}{dr^2} + \frac{2l}{r} \frac{d}{dr} - \frac{2l}{r^2} \right] + qV_s(r) \pm \delta_{q,-1}K + V_p(r) - \varepsilon\right] f_l(r) = 0, \quad (4)$$

with

$$Kf_l = F_l(r) = \frac{4\pi}{2l+1} \varphi_0(r) \left[ (\varepsilon_0 - \varepsilon) \delta_{l,0} r \int_0^{\infty} \varphi_0(x) f_l(x) x dx + r^{-2l} \int_0^r \varphi_0(x) f_l(x) x^{2l+1} dx + r \int_r^{\infty} \varphi_0(x) f_l(x) dx \right]. \quad (5)$$

Here,  $\varepsilon_0$  is the ground-state energy of the isolated target atom ( $\varepsilon_0 < 0$ ) and  $\varphi_0$  is the unperturbed Hartree-Fock atomic orbital of the target taken from Ref. 21. The integrals in Eq. (5) can be eliminated by differentiation:

$$\left\{ -\frac{d^2}{dr^2} + 2 \left[ \frac{\varphi_0'}{\varphi_0} - \frac{l}{r} \right] + \left[ \frac{\varphi_0''}{\varphi_0} - 2 \left( \frac{\varphi_0'}{\varphi_0} \right)^2 + \frac{2l}{r^2} \left( \frac{\varphi_0'}{\varphi_0} r + 1 \right) \right] \right\} F_l(r) = 4\pi \varphi_0^2 f_l(r), \quad (6)$$

with the boundary conditions

$$F_l(0) = 0,$$

$$F_l'(0) = \frac{4\pi}{2l+1} \varphi_0(0) \int_0^{\infty} [\delta_{l,0}(\varepsilon_0 - \varepsilon)x + 1] \varphi_0(x) f_l(x) dx. \quad (6a)$$

The  $\delta_{l,0}$  term ensures the orthogonality of the scattering wave to the target orbital. Equation (6), together with Eq. (4), are solved simultaneously by numerical integration, using the routines DIFFSYS.<sup>22</sup> Iterations are required to obtain the self-consistency in the second boundary condition. Frequently, four iterations are sufficient, and five-figure accuracy in the eigenvalue or phase shift is achieved without complications for any of the trial polarization potentials used. This procedure amounts to using the exact static exchange potential for all the electronic systems studied here.

### B. Polarization potentials

The well-known asymptotic form of the polarization potential  $V_p$  in Eq. (1) has the leading term  $-\alpha_d/2r^4$  and the next important term  $-(\alpha_q - 6\beta_1)/2r^6$ , where  $\alpha_d$  and  $\alpha_q$  are the dipole and quadrupole polarizabilities, respectively, and  $\beta_1$  the first nonadiabatic correction term.  $\beta_1$  is known for several atoms<sup>23,24</sup> and tends to cancel the quad-

TABLE I. Systems and the reference values chosen for evaluation of model polarization potentials.

Systems	State	Reference values
$e^+ - \text{H}$	Scattering	Scattering length $a_s = -2.1036a_0^a$
$e^- - \text{H}$	Singlet scattering	Scattering length $a_s = 5.965a_0^b$
	Singlet bound	Binding energy $\varepsilon = -0.027717 \text{ a.u.}^c$
	Triplet scattering	Scattering length $a_s = 1.7686a_0^b$
$e^+ - \text{He}$	Scattering	Scattering length $a_s = -0.472a_0^d$
$e^- - \text{He}$	Doublet scattering	Scattering length $a_s = 1.1835a_0^e$
$e^- - \text{He}^+$	$^1S, ^1P,$ $^3S, ^3P$	Atomic energy levels <sup>f</sup>
$e^- - \text{Li}^+$	$^2S, ^2P, ^2D$	Atomic energy levels <sup>f</sup>

<sup>a</sup>Reference 14.

<sup>b</sup>Reference 15.

<sup>c</sup>Reference 16.

<sup>d</sup>Reference 17.

<sup>e</sup>Reference 18.

<sup>f</sup>References 19 and 20.

ruple polarization potential. For the atomic hydrogen target, an additional energy-dependent contribution is found in an  $r^{-6}$  term.<sup>25</sup> Since the contribution from the  $r^{-6}$  term is less important, we use only the dipole term and expect the cutoff function to represent all other contributions. The dipole polarizabilities of hydrogen and  $\text{He}^+$  are known from elementary theory. We use the accurate values  $1.383a_0^3$  for helium<sup>26</sup> and  $0.1894a_0^3$  for  $\text{Li}^+$ .<sup>27</sup>

Our model polarization potential is thus

$$V_p(r) = -\frac{\alpha_d}{2} \frac{1}{r^4} w\left(\frac{r}{\rho}\right). \quad (7)$$

The cutoff function  $w$  is either from the literature<sup>5-9,28-40</sup> or is taken to be

$$w(\xi) = (1 - e_n^\xi e^{-\xi})^m, \quad (8)$$

where  $m$  is either 1, 2, or 4 and  $e_n$  is the truncated exponential function:

$$e_n^\xi = \sum_{i=0}^n \frac{\xi^i}{i!}. \quad (9)$$

$\rho$  in the cutoff function is the adjustable parameter. Since it strongly depends on the values of  $n$  and  $m$ , a new parameter, an effective radius  $r_0$ , which is insensitive to  $n$  and  $m$  values, is useful. We take  $r_0$  to be the equivalence point in the cutoff function, i.e.,

$$\int_0^{r_0} w\left(\frac{r}{\rho}\right) dr = \int_{r_0}^{\infty} \left[1 - w\left(\frac{r}{\rho}\right)\right] dr, \quad (10)$$

which works out to be

$$r_0 = \begin{cases} (n+1)\rho & \text{for } m=1, \\ (1.0952n + 1.8556)\rho & \text{for } m=2, \\ (1.2597n + 2.3502)\rho & \text{for } m=4 \end{cases} \quad (11)$$

for the cutoffs given by Eq. (8). The cutoff functions generally have the shape shown in Fig. 1, and Eq. (10) is equivalent to selecting  $r_0$  so that the areas of the two shaded regions are equal.

The cutoff function defined by Eq. (8) was previously used in the dipole polarization potential with  $m=1$  and  $n=5$  and in a quadrupole polarization potential with  $m=1$  and  $n=7$  by Laurenzi,<sup>41</sup> and in a polarization potential with  $m=1$  and  $n=4$  and 5 by Valiron *et al.*<sup>36</sup> The cutoff functions derived from a semiempirical analysis of the optical potential<sup>39,42</sup> are numerically very close to our cutoff function with  $m=2$  and  $n=3$ . A similar cutoff function is also used to model nonadiabatic effects in positron-atom collisions.<sup>43</sup>

The cutoff functions given by Eq. (8) have the following short- and long-range behaviors:

$$\lim_{\xi \rightarrow 0} w(\xi) = \left[ \frac{\xi^{n+1}}{(n+1)!} \right]^m, \quad (12)$$

$$\lim_{\xi \rightarrow \infty} w(\xi) = 1.$$

The second property ensures that the model polarization

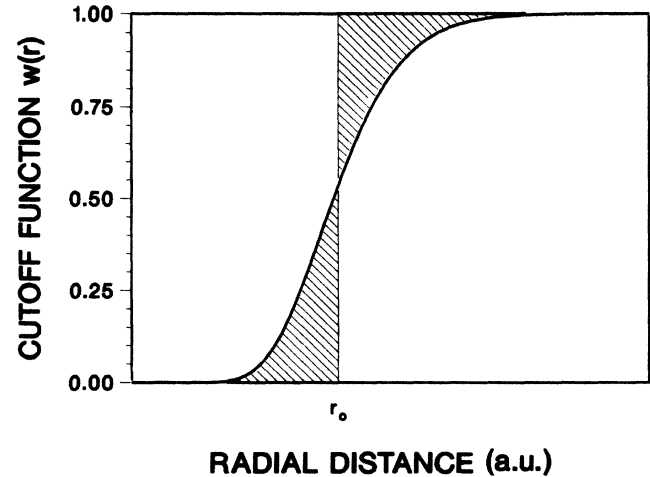


FIG. 1. A representative cutoff function, showing how  $r_0$ , the effective target radius, is defined so as to make the two shaded areas equal. [The actual cutoff shown above is that given by Eq. (8) with  $m=2$  and  $n=8$ .]

potential gives the well-known correct long-range behavior of the dipole term. From the short-range behavior of the cutoff function, it is necessary for  $n$  to be greater than or equal to 4 for  $m=1$ , 2 for  $m=2$ , and 1 for  $m=4$  in order to have a finite polarization potential at the origin. In the present work,  $n$  is varied from 4 to 14 for  $m=1$ , from 2 to 14 for  $m=2$ , and from 2 to 4 for  $m=4$ . The other common cutoff functions tested in this work are the following. From Buckingham,<sup>5-8,28</sup>

$$w(\xi) = \xi^4 / (\xi^4 + 1)^2, \quad r_0 = \frac{3}{4}\pi\rho.$$

From Bethe and Reeh,<sup>2,29-31</sup>

$$w(\xi) = 1 - \frac{1}{3}e^{-2\xi}(1 + 2\xi + 6\xi^2 + \frac{20}{3}\xi^3 + \frac{4}{3}\xi^4) - \frac{2}{3}e^{-4\xi}(1 + \xi)^4, \quad r_0 = 2.5365\rho.$$

From Callaway and Temkin,<sup>2,32</sup>

$$w(\xi) = 1 - e^{-2\xi}(1 + 2\xi + 2\xi^2 + \frac{4}{3}\xi^3 + \frac{2}{3}\xi^4 + \frac{4}{27}\xi^5), \quad r_0 = \frac{25}{9}\rho.$$

From Takayanagi and Geltman,<sup>9,33,34</sup>

$$w(\xi) = \begin{cases} \xi^4 & \text{if } \xi < 1, \\ 1 & \text{otherwise,} \end{cases} \quad r_0 = \frac{4}{5}\rho. \quad (13)$$

From Lane and Geltmann,<sup>35-38</sup>

$$w(\xi) = 1 - e^{-\xi^6}, \quad r_0 = 0.9277\rho.$$

From Taylor, Wang, and Yaris,<sup>39</sup>

$$w(\xi) = [1 - e^{-\xi}(1 + \xi + \frac{1}{2}\xi^2 + \frac{1}{8}\xi^3)]^2, \quad r_0 = 4.8340\rho.$$

From Gianturco and Thompson,<sup>37,40</sup>

$$w(x) = (1 - e^{-x})^6, \quad r_0 = \frac{49}{20}\rho.$$

TABLE II. The effective radii in various trial polarization potentials given by Eqs. (7) and (8), which reproduce the reference values listed in Table I. The effective radius is related to the cutoff parameter  $\rho$  by Eq. (10). The ratios of H are calculated from the average of the two  $r_0^S$  values.

Types of cutoff functions	Hydrogen target						Helium target		
	$e^+ \text{-H}$ scatt. $r_0^+$	Effective radii		$e^- \text{-H}$ triplet scatt. $r_0^T$	$r_0^S/r_0^+$	$r_0^T/r_0^S$	$e^+ \text{-He}$ scatt. $r_0^+$	$e^- \text{-He}$ doublet scatt. $r_0^D$	$r_0^D/r_0^+$
		$e^- \text{-H}$ singlet scatt. $r_0^S$	$e^- \text{-H}$ singlet bound $r_0^S$						
Buckingham	3.207	4.208	4.163	5.770	1.306	1.378	2.252	4.109	1.817
Bethe-Reeh	2.141	2.384	2.394	4.591	1.116	1.921	1.562	2.569	1.644
Callaway-Temkin	2.164	2.475	2.475	4.642	1.144	1.875	1.575	2.686	1.705
Takayanagi-Geltman	1.914	1.944	1.966	4.502	1.021	2.302	1.415	2.481	1.753
Lane-Geltman	1.896	1.864	1.891	4.347	0.990	2.315	1.404	2.386	1.700
Wang-Taylor-Yaris	2.105	2.298	2.306	4.554	1.094	1.979	1.542	2.490	1.617
Gianturo-Thompson	2.244	2.595	2.590	4.677	1.155	1.804	1.627	2.705	1.663
$m=1$ $n=4$	2.188	2.529	2.525	4.650	1.155	1.840	1.591	2.730	1.716
$n=5$	2.117	2.342	2.348	4.584	1.107	1.955			
$n=6$	2.070	2.226	2.238	4.515	1.078	2.034	1.517	2.444	1.611
$n=7$	2.036	2.147	2.162	4.455	1.058	2.068			
$n=8$	2.010	2.089	2.108	4.400	1.044	2.097	1.480	2.362	1.596
$n=9$	1.991	2.045	2.066	4.344	1.032	2.113			
$n=10$	1.975	2.011	2.033	4.292	1.024	2.123	1.456	2.341	1.607
$n=11$	1.962	1.984	2.006	4.234	1.071	2.127			
$n=12$	1.952	1.960	1.985	4.199	1.010	2.129	1.440	2.340	1.625
$n=13$	1.943	1.942	1.967	4.137	1.006	2.117			
$n=14$	1.935	1.926	1.952	4.103	1.002	2.116	1.430	2.346	1.641
$n=\infty$	1.837	1.731	1.764	3.161	0.979	1.809	1.364	2.433	1.784
$m=2$ $n=2$	2.224	2.504	2.507	4.746	1.126	1.894	1.621	2.669	1.647
$n=3$	2.092	2.240	2.253	4.529	1.074	2.016	1.535	2.438	1.589
$n=4$	2.024	2.107	2.125	4.390	1.045	2.075	1.489	2.356	1.582
$n=5$	1.983	2.028	2.049	4.277	1.028	2.098	1.461	2.328	1.593
$n=6$	1.957	1.955	2.000	4.188	1.015	2.107	1.445	2.322	1.608
$n=7$	1.939	1.941	1.965	4.110	1.008	2.104	1.432	2.326	1.624
$n=8$	1.926	1.916	1.941	4.040	1.001	2.095	1.424	2.332	1.638
$n=9$	1.918	1.896	1.922	3.981	0.995	2.085	1.418	2.340	1.650
$n=10$	1.912	1.882	1.902	3.924	0.991	2.071	1.413	2.348	1.661
$n=11$	1.907	1.870	1.897	3.875	0.987	2.058	1.411	2.358	1.671
$n=12$	1.902	1.860	1.889	3.830	0.985	2.044	1.409	2.365	1.679
$n=13$	1.900	1.854	1.881	3.790	0.982	2.030	1.407	2.371	1.685
$n=14$	1.899	1.846	1.875	3.754	0.979	2.018	1.406	2.379	1.692
$n=\infty$	1.837	1.731	1.764	3.161	0.979	1.809	1.364	2.433	1.784
$m=4$ $n=2$	2.013	2.089	2.104	4.340	1.041	2.072	1.480	2.326	1.571
$n=3$	1.961	1.984	2.007	4.206	1.050	2.107	1.447	2.309	1.596
$n=4$	1.939	1.934	1.960	4.126	1.004	2.119	1.432	2.325	1.623

### III. RESULTS AND DISCUSSIONS

#### A. Relationships among various effective radii

The reference values<sup>4-20</sup> used in our work to determine the parameter  $\rho$  are listed in Table I. Values of the effective radius  $r_0$ , which is related to  $\rho$  by Eq. (10), are adjusted to reproduce these values and are listed in Table II for the  $e^\pm\text{-H}$  and  $e^\pm\text{-He}$  systems for various polarization potentials. The Bethe-Reeh and Callaway-Temkin potentials were originally derived for one-electron targets, and have no adjustable parameters in their cutoff functions. We have used only the dipole terms of their potentials, and replaced  $r$  by  $r/\rho$  in their cutoff functions.  $n = \infty$  indicate

that a step function is used for the cutoff function.

We find the following regularities: The adjusted effective radius for the electron triplet scattering from atomic hydrogen ( $r_0^T$ ) is approximately 2 times larger than that for singlet scattering ( $r_0^S$ ) and that for the bound state for all polarization potential studied, except the Buckingham potential; and the effective radius for the positron scattering ( $r_0^+$ ) is about the same as  $r_0^S$ . Although the difference is insignificant, we take  $r_0^S$  as an average value of those for singlet scattering and bound states. The extend of these regularities is shown by the last two columns under "Hydrogen target" in Table II. Generally, the polarization potential given by Eq. (8) with a larger  $n$  value gives

TABLE III. Effective radii in the cutoff function [Eq. (8)] with  $m=2$  and  $n=8$  which reproduce the best atomic He energy levels listed as reference values. The  $D$  states are insensitive to the effective radius.

States	Electronic configuration	Reference values (a.u.)	Effective radii of He <sup>+</sup> ( $a_0$ )
<sup>1</sup> S	1s <sup>2</sup>	-0.903 570	0.879
	1s2s	-0.145 981	0.810
	1s3s	-0.061 290	0.796
	1s4s	-0.033 609	0.782
<sup>1</sup> P	1s2p	-0.123 849	1.396
	1s3p	-0.055 164	1.332
	1s4p	-0.031 092	1.260
<sup>3</sup> S	1s2s	-0.175 239	1.795
	1s3s	-0.068 708	1.675
	1s4s	-0.036 534	1.515
<sup>3</sup> P	1s2p	-0.133 176	1.491
	1s3p	-0.058 101	1.446
	1s4p	-0.032 347	1.392

better phase shifts for positronic systems, while the polarization potential with a smaller  $n$  value produces better phase shifts for electronic systems and a smaller difference in the effective radii for singlet scattering and bound states.

For the helium target, the effective radii which produce the best scattering lengths for electron and positron scattering are also listed in Table II. The last column shows the ratios of the effective radii for electron scattering from a helium atom,  $r_0^D$ , to those for positron scattering off helium,  $r_0^+$ ; the regularity of this ratio, regardless of the cutoff functions, is apparent.

The atomic helium energy levels are calculated as the electron binding energies to the He<sup>+</sup> core. Only the results from the cutoff function with  $m=2$  and  $n=8$  are presented in Table III, since the results are very much the same for all other cutoff functions studied. This choice of cutoff function is made because the square root of cutoff function is needed in the future (for the calculation of positronium formation cross sections), which means we want  $m=2$ ; and because the  $r_0^S/r_0^+$  ratio (Table II) is closest to unity for  $n=8$ . Table III shows the best effective radius for each electronic configuration using this cutoff. The reference energy levels are taken from the experimental values tabulated by Moore,<sup>19</sup> and the ionization potentials are taken from Ref. 20. As seen from the table, similar electronic configurations seem to have similar effective radii, although they become slightly smaller for the higher excited states. A comparison of the effective radii for the <sup>1</sup>S states with those for the <sup>3</sup>S states tells again that the  $r_0$  ratios of the triplet over the singlet states are around 2. The singlet and triplet  $P$  states give rise to similar  $r_0$  values somewhere between those for the singlet and the triplet  $S$  states. We have also calculated singlet and triplet  $D$  states. They are, however, not sensitive to the effective radius.

Similarly, that atomic lithium energy levels are calculated as electronic binding to the Li<sup>+</sup> core. The effective

TABLE IV. Effective radii in the cutoff function [Eq. (8)] with  $m=2$  and  $n=8$  which reproduce the best atomic Li energy levels listed as reference values. The  $D$  states are less sensitive to the effective radius.

States	Electronic configuration	Reference values (a.u.)	Effective radii of Li <sup>+</sup> ( $a_0$ )
<sup>2</sup> S	1s <sup>2</sup> 2s	-0.198 142	1.227
	1s <sup>2</sup> 3s	-0.074 182	1.184
	1s <sup>2</sup> 4s	-0.038 615	1.180
<sup>2</sup> P	1s <sup>2</sup> 2p	-0.130 235	1.177
	1s <sup>2</sup> 3p	-0.057 236	1.166
	1s <sup>2</sup> 4p	-0.031 975	1.157
<sup>2</sup> D	1s <sup>2</sup> 3d	-0.055 606	~1.9
	1s <sup>2</sup> 4d	-0.031 274	~1.8

radii which reproduce the experimentally determined energy levels<sup>19,20</sup> are listed in Table IV. Although the same tendency is observed in the effective radii, the  $r_0$  values for doublet  $P$  states are very close to those for doublet  $S$  states.  $r_0$  values for doublet  $D$  states have less significance since  $D$  states are only slightly affected by the polarization potential. In our calculations, the change of  $r_0$  from 1.6 to 1.0 generates only 0.01% difference in energy from the reference values.

#### B. The difference between electron and positron polarization potentials

The difference in the polarization potentials which give the best results for electronic and positronic systems has been noticed for some time, as mentioned in Sec. I. In addition to the difference created by a positively or negatively charged particle, the opposite sign in the exchange potential for singlet and triplet states for the  $e^-$ -H systems makes a difference in the dynamic term. Recently, Câmpeanu<sup>34</sup> has also adopted the above idea to explain

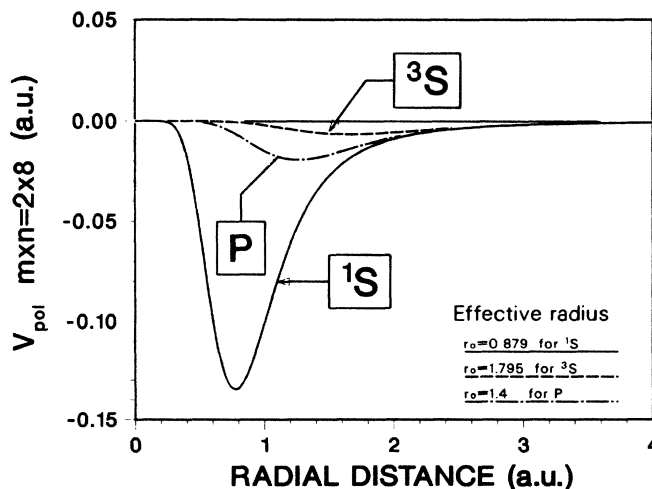


FIG. 2. The polarization potentials using the cutoff function given by Eq. (8) with  $m=2$  and  $n=8$ , which produce the best atomic helium energy levels for singlet and triplet  $S$  states and for  $P$  states. (See Table III.)

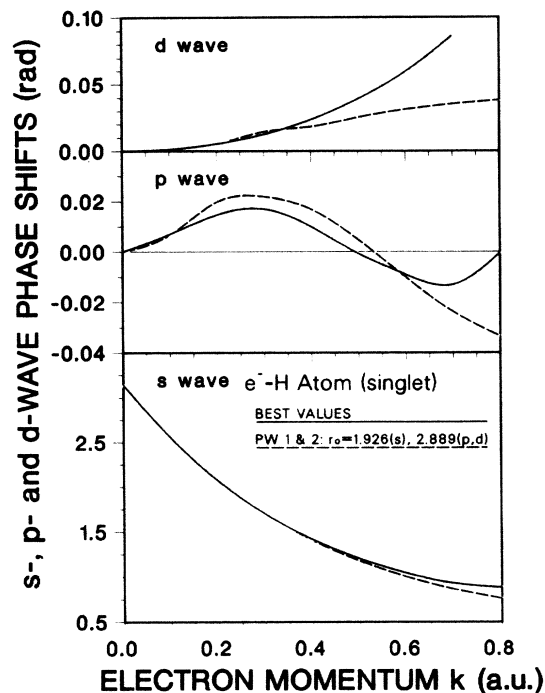


FIG. 3. The  $s$ -,  $p$ -, and  $d$ -partial-wave phase shifts of an electron scattering from a hydrogen atom (single state). Best values are taken from Ref. 15 for  $s$ -wave, from Ref. 44 for  $p$ -wave, and from Ref. 45 for  $d$ -wave phase shifts. PW1 denotes that effective radii for electronic systems are obtained from the corresponding positronic effective radius using the relations given in Table V, and PW2, vice versa. PW1 and PW2 are plotted as a single curve because they are indistinguishable on the scale shown.

different  $r_0$  values in the Takayanagi-Geltman polarization potential used for positron- and electron-helium scattering calculations. His  $r_0^D/r_0^+$  ratio, 1.5, differs from our ratio by 14%, and is probably due to the exchange approximation employed in his calculations and to the different reference value chosen.

As shown in Fig. 2, the difference in polarization potentials for electron- $\text{He}^+$  interactions is, however, much larger than one would expect from assuming that the omitted dynamic term ( $\beta_1$ ) can be compensated for by omitting the quadrupole polarization potential ( $\alpha_q$ ).<sup>13</sup> The short-range importance of these terms is evident. Our preliminary investigation in using the cutoff functions proposed by Wang *et al.*<sup>39</sup> shows that the inclusion of a quadrupole term makes the total polarization potential only about 6% deeper at the minimum point and has practically no effect at  $r$  larger than  $4a_0$  for  $e^+$ -He scattering. Thus we would like to consider the differences from another point of view.

It is clear from Fig. 2 that the main difference between electron-core interactions in the singlet and triplet states arises from the Pauli exclusion effect. In the triplet state an incident electron cannot penetrate into the core region, causing a large effective radius in the polarization potential. On the other hand, for the singlet state, an incident electron can penetrate without violating the exclusion principle. Since there is no exclusion in positronic sys-

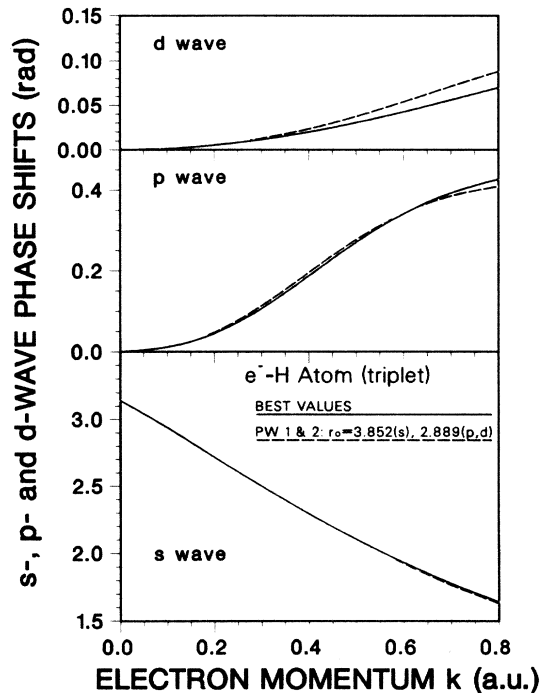


FIG. 4. The  $s$ -,  $p$ -, and  $d$ -partial-wave phase shifts of an electron scattering from a hydrogen atom (triple state). Best values are taken from Ref. 15 for  $s$ -wave, from Ref. 44 for  $p$ -wave, and from Ref. 45 for  $d$ -wave phase shifts. Values of the effective radius are calculated from the relations given in Table V. PW1 and PW2 are plotted as a single curve because they are indistinguishable on the scale shown.

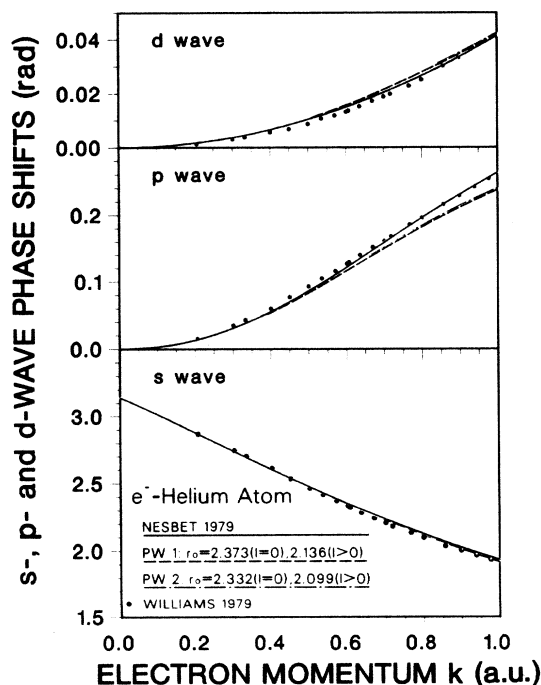


FIG. 5. The  $s$ -,  $p$ -, and  $d$ -partial-wave phase shifts of an electron scattering from a helium atom. Best theoretical values are taken from Ref. 18. The best experimentally determined partial-wave phase shifts taken from Ref. 46 are also shown. The values of the effective radius are calculated from the relations given in Table V.

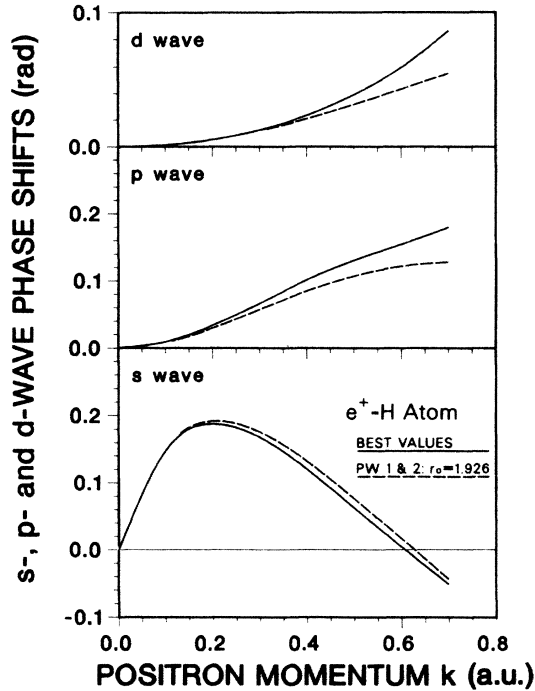


FIG. 6. The  $s$ -,  $p$ -, and  $d$ -partial-wave phase shifts of a positron scattering from a hydrogen atom. Best values are taken from Ref. 47 for  $s$ -wave, from Ref. 48 for  $p$ -wave, and from Ref. 45 for  $d$ -wave phase shifts. PW1 and PW2 are plotted as a single curve because they are indistinguishable in the scale shown.

tems, we also expect a similar effective radius to that for the corresponding singlet electronic system.  $r_0^+$ 's are indeed very close to  $r_0^S$ 's, although small differences are observed (sixth column of Table II) which may account for the difference in the dynamic terms as explained previously. As already noted, the effective radius for the triplet state,  $r_0^T$ , is close to twice that for the corresponding singlet and positronic states (seventh column of Table II). Thus, for one-electron targets, we propose the parametrization

$$r_0^T = 2r_0^S = 2r_0^+ \quad (14)$$

The doublet systems considered here have two electrons in the target. Adding an outer electron gives three electrons, from which three pairs can be chosen. Since the particles are indistinguishable, the pairs must be also. One of these has parallel spins (necessarily triplet) and two, opposite (half singlet and half triplet). Thus the singlet:triplet character of the pairs is 1:2, and we might sensibly take the effective doublet radius to be the weighted mean,

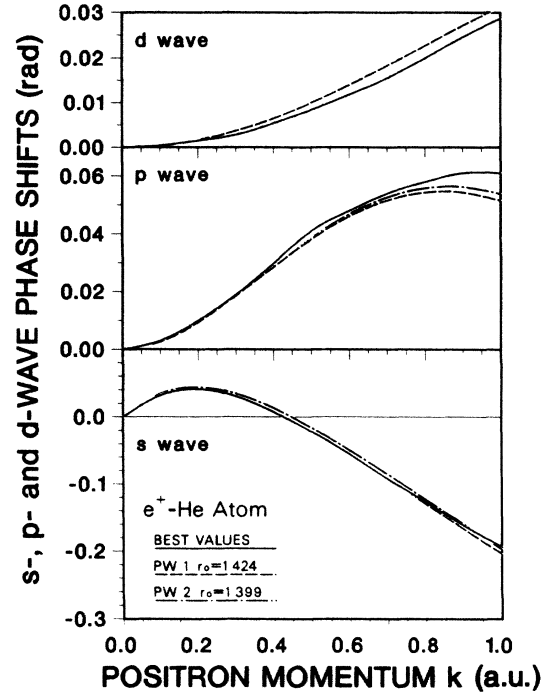


FIG. 7. The  $s$ -,  $p$ -, and  $d$ -partial-wave phase shifts of a positron scattering from a helium atom. Best values are taken from Ref. 17 for  $s$ -wave and from Ref. 49 for  $p$ -wave phase shifts. Best values for  $d$ -wave phase-shifts are read from Fig. 11 (Ref. 50) in Ref. 51.

$$r_0^D = \frac{r_0^S + 2r_0^T}{3} = \frac{5}{3}r_0^+ \quad (15)$$

which is very close to the values tabulated in the last column in Table II.

The results of the atomic energy-level calculations are listed in Tables III and IV. We have no positronic reference values for  $\text{He}^+$  and  $\text{Li}^+$  from which to determine  $r_0^+$ , but we see from the  $^1S$  and  $^3S$  results in Table III that  $r_0^T$  is indeed twice  $r_0^S$ . That is, Eq. (14) evidently works for  $\text{He}^+$  as for H, so  $r_0^+$  is thus determined. With some confidence, therefore, we find  $r_0^+$  for  $\text{Li}^+$  from Eq. (15) with  $r_0^D$  from the  $^2S$  results of Table IV.

We propose that the effective radius of one- and two-electron targets for non- $S$  states be three halves of the corresponding  $r_0^+$ . This gives  $r_0 = 1.1$  for both  $^2P$  and  $^2D$  states. The agreement (see Table IV) is good for the  $^2P$  states but not for the  $^2D$  states. However, the  $^2D$  energies of Li are very insensitive to the effective radius, and  $\frac{2}{3}r_0^+$  gives quite reasonable  $d$ -wave phase shifts in electron-hydrogen and -helium scattering calculations, as seen

TABLE V. Proposed relationships between effective radii in model polarization potentials for positronic and electronic systems.

Angular momentum	$e^+ \text{-H and } e^+ \text{-He systems}$	$e^- \text{-H and } e^- \text{-He systems}$		
		Singlet	Doublet	Triplet
$l=0$	$r_0^+$	$r_0^S = r_0^+$	$r_0^D = \frac{r_0^S + 2r_0^T}{3} = \frac{5}{3}r_0^+$	$r_0^T = 2r_0^S = 2r_0^+$
$l \geq 1$	$r_0^+$	$\frac{3}{2}r_0^+$	$\frac{3}{2}r_0^+$	$\frac{3}{2}r_0^+$

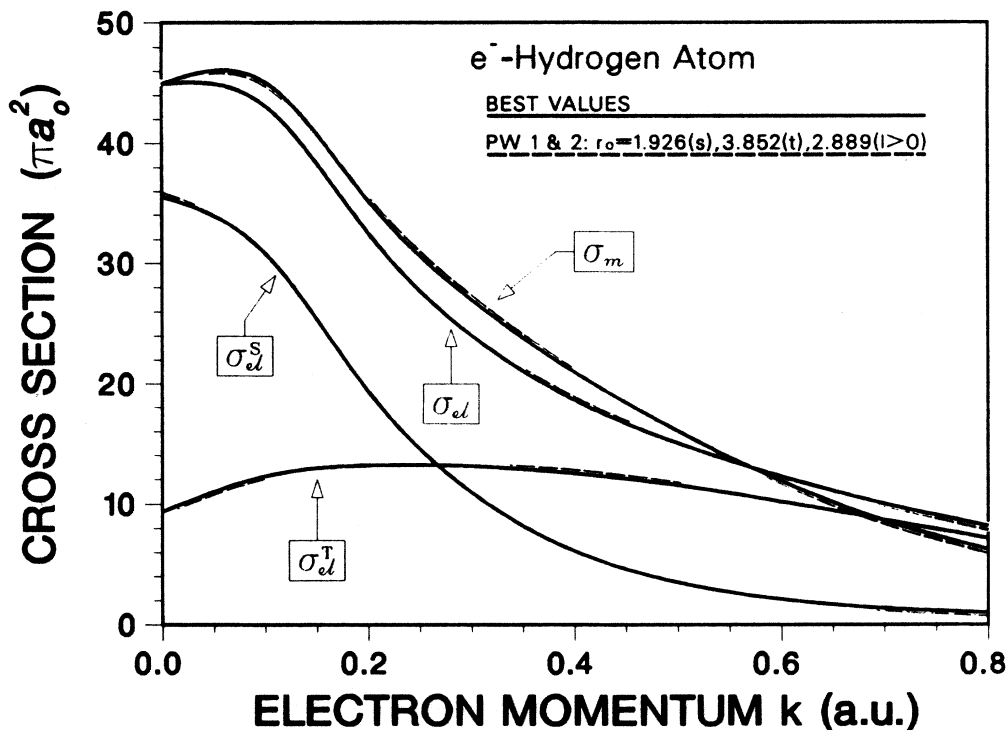


FIG. 8. Total cross sections ( $\sigma_{el}$ ) and momentum-transfer cross sections ( $\sigma_m$ ) of an electron elastically scattered from a hydrogen atom. The contributions from the singlet and triplet states are shown as  $\sigma_{el}^S$  and  $\sigma_{el}^T$ , respectively. Best values are calculated from  $s$ -,  $p$ -, and  $d$ -wave phase shifts (Refs. 15, 44, and 45). (See Figs. 3 and 4). The contributions from higher ( $l \geq 3$ ) partial waves are estimated from the Born approximation with the equations given in Ref. 18.

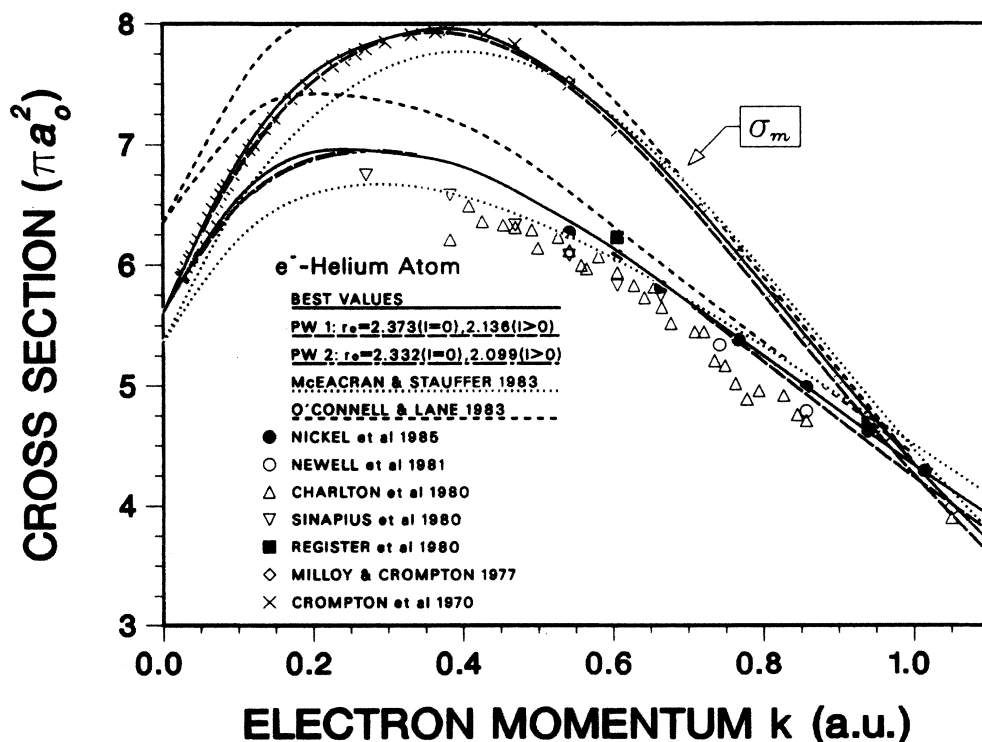


FIG. 9. Total cross sections ( $\sigma_{el}$ ) and momentum-transfer cross sections ( $\sigma_m$ ) of an electron elastically scattered from a helium atom. Best values are calculated from  $s$ -,  $p$ -, and  $d$ -wave phase shifts (Ref. 18). (See Fig. 5). Total and momentum-transfer cross sections calculated from the polarized orbital method (Ref. 13) and the model potential method (HCO model) (Ref. 52) are also shown. Experimental values are taken from Ref. 53–59.

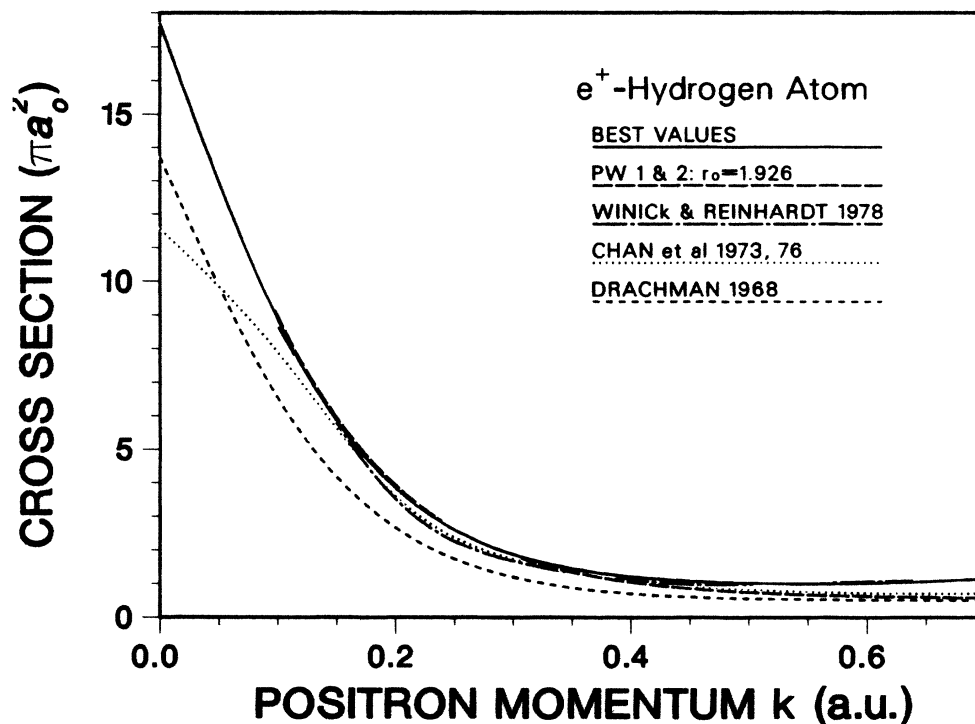


FIG. 10. Total cross sections of a positron elastically scattered from a hydrogen atom. Calculated momentum-transfer cross sections (not shown to avoid excessive cluttering of the graph) are also very close to low energies, and deviate slightly at near the positronium formation threshold. Best values are calculated from  $s$ - (Ref. 47),  $p$ - (Ref. 48), and  $d$ -wave (Ref. 45) phase shifts (see Fig. 2). Results from other theoretical calculations are also shown (Refs. 11 and 60–64). The values of Chan *et al.* are calculated from  $s$ - (Ref. 61),  $p$ - (Ref. 62), and  $d$ -wave (Ref. 63) phase shifts. The values of Drachman are calculated from  $s$ -,  $p$ - (Ref. 11), and  $d$ -wave (Ref. 64) phase shifts.

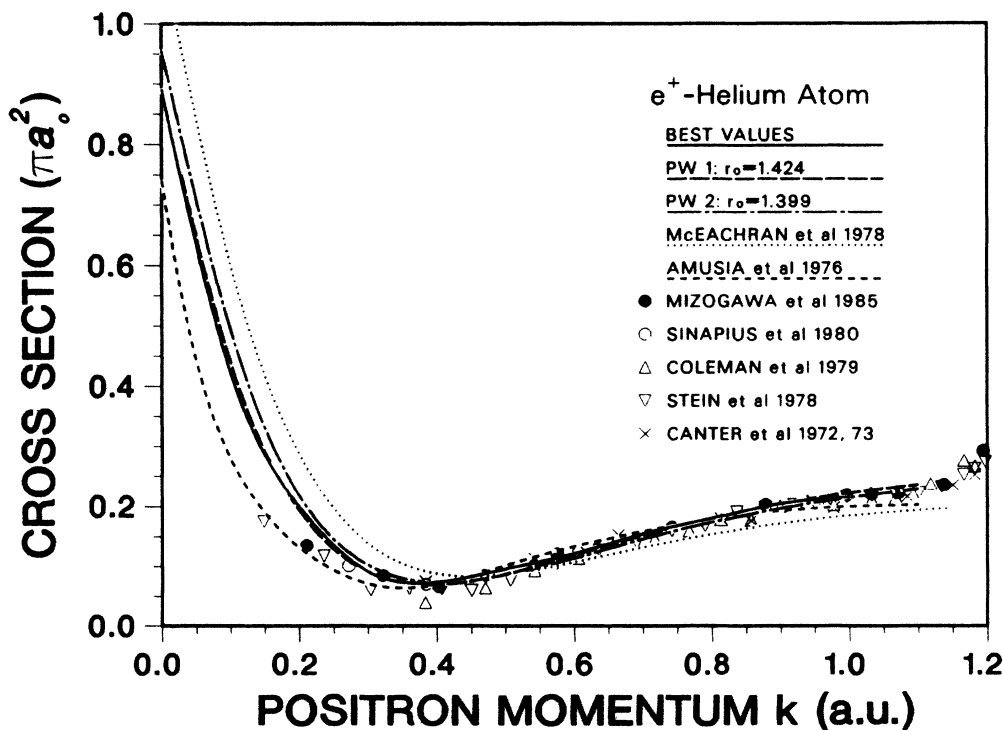


FIG. 11. Total cross sections of a positron elastically scattered from a helium atom. Both momentum-transfer cross sections calculated from the PW1 and PW2 methods (not shown) are very close to the best theoretical values. The best values are calculated from  $s$ - (Ref. 17),  $p$ - (Ref. 49), and  $d$ -wave (Ref. 50) phase shifts. (See Fig. 6.) Those values are very close to the total cross sections shown in Ref. 65. Other theoretical results, of McEachran *et al.* (Ref. 66) and Amusia *et al.* (Ref. 67), are also shown. Experimental values are taken from Refs. 68–71.

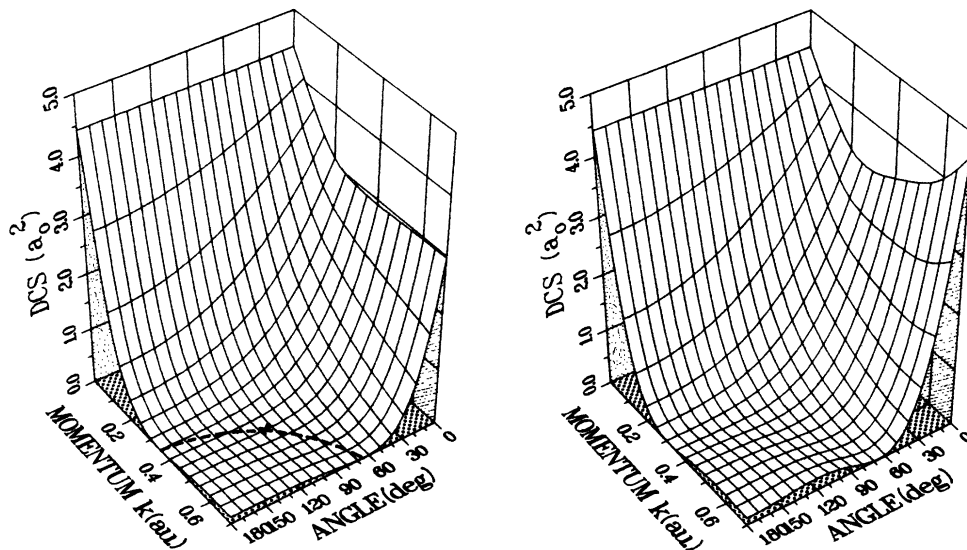


FIG. 12. Differential cross sections (DCS's) of a positron elastically scattered from a hydrogen atom (left, present work; right, best values). The cutoff function with  $m=2$  and  $n=8$  and  $r_0^+ = 1.926$  is used. The dashed curve and the  $\times$  represent the locus of the differential cross-section minima and the critical point. Best values are calculated from  $s$ -,  $p$ -, and  $d$ -wave phase shifts from Refs. 47, 48, and 45, respectively.

from Figs. 3–5. For positronic systems, previous calculations<sup>9</sup> have shown that the same effective radius produces good results in  $s$ -,  $p$ -, and  $d$ -wave phase-shift calculations. We have also confirmed this by using various trial polarization potentials for positron-scattering calculations from both hydrogen and helium, as seen from Figs. 6 and 7.

The relations which we have found between the effective radii for positronic and electronic systems are summarized in Table V. By using these relations we have calculated partial-wave phase shifts (as shown in Figs. 3–7) and total and momentum-transfer cross sections of positron and electron elastic scatterings from atomic hydrogen and helium. The symbol PW1 in the figures indicates

that the effective radii for electronic systems are obtained from the corresponding positronic effective radius using the relations in Table V, and PW2, vice versa. Our elastic total cross sections and momentum-transfer cross sections are compared with the theoretical values and recent experimental values<sup>14,15,17–19,44–71</sup> in Figs. 8–11. The contributions from the higher ( $l \geq 3$ ) partial waves are taken into account using the Born approximation with the equations given in Ref. 18. Total cross sections calculated from the PW1 and PW2 methods are in excellent agreement with the best values are shown in Figs. 8–11, although our calculation does not reproduce the very shallow Ramsauer minimum in positron-hydrogen scattering.

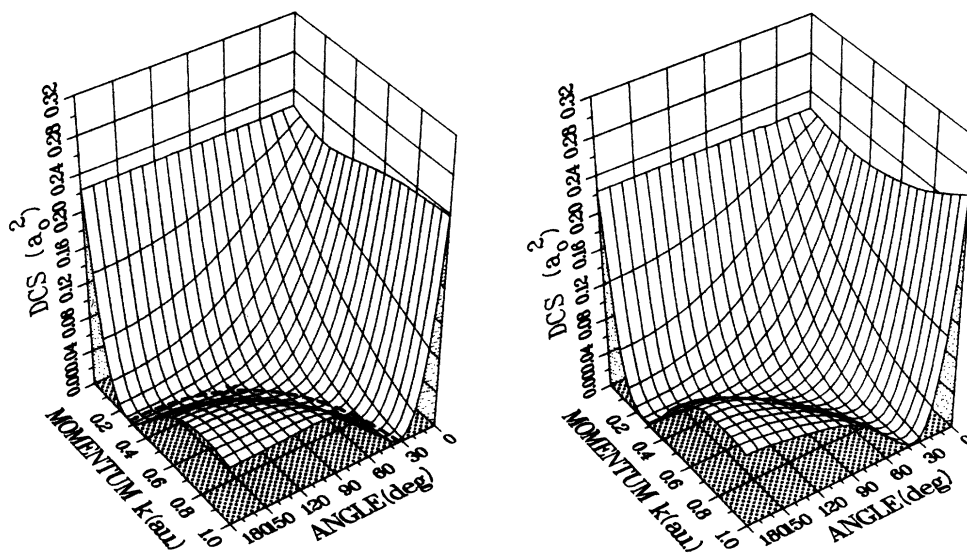


FIG. 13. Differential cross sections of a positron elastically scattered from a helium atom (left, present work; right, best values). The cutoff function with  $m=2$  and  $n=8$  and  $r_0^+ = 1.424$  is used. The dashed curve and the  $\times$  represent the locus of the differential cross-section minima and the critical point. Best values are calculated from  $s$ -,  $p$ -, and  $d$ -wave phase shifts from Refs. 17, 49, and 50, respectively.

Since electron scattering is less sensitive to the polarization potential than positron scattering,<sup>10</sup> PW1 always gives better agreement than PW2 if an accurate positronic reference value is available. Since far more is known about electron scattering, PW2 may be a useful method with which to investigate the corresponding positronic systems.

Differential cross sections are calculated from the *s*-, *p*-, and *d*-wave phase shifts of the PW1 method. Since contributions from the higher partial waves is significant, as demonstrated by Williams,<sup>72</sup> they are included using the modified effective range formula of O'Malley, Spruch, and Rosenberg<sup>73</sup> and the closed form of Thompson.<sup>74</sup> Our results of the differential cross sections for the electronic systems are in very good agreement with the best theoretical results. The results for the positronic systems are shown in Figs. 12 and 13. Differential cross-section measurements for positron-hydrogen and -helium have not been yet reported. Our results again show excellent agreement with the best values at low energies. Near the Ps formation threshold, our differential cross sections for the positronic systems exhibit a noticeable difference from the best results at small scattering angles, as expected from the lack of the Ps formation channel in our calculations.

Recently, Wahedra *et al.*<sup>75</sup> reported an interesting demonstration on minima (critical points) in the differential cross sections of a positron scattering from Ar, Kr, and Xe. Their simple approximation gives critical angle being  $2 \arctan \sqrt{2} \approx 109.5^\circ$ . As shown in Fig. 14, we found, for positron-hydrogen scattering, that the critical angle ( $\theta_{cr}$ ) is  $105.0^\circ \pm 0.25^\circ$ , the critical incident momentum ( $k_{cr}$ ) is  $(0.450 \pm 0.013)a_0^{-1}$ , and the critical differential cross section ( $I_{cr}$ ) is  $(3.7 \times 10^{-5})a_0^2$ ; and for helium,  $\theta_{cr} = 100.0^\circ \pm 0.25^\circ$ ,  $k_{cr} = (0.350 \pm 0.013)a_0^{-1}$ , and  $I_{cr} = (3.8 \times 10^{-7})a_0^2$ . These values are similar to those obtained by Wahedra *et al.*<sup>75</sup> for Ar, Kr, and Xe using phase shifts from polarized orbital calculations.<sup>76</sup> Since the contributions from the higher partial waves are less significant for small target atoms, the critical angles for hydrogen and helium are closer to  $109.5^\circ$  than those for Ar, Kr, and Xe.

#### IV. CONCLUSIONS AND FUTURE WORK

We have performed calculations of low-energy electrons and positrons scattering elastically from atomic hydrogen and helium and of electrons binding to  $\text{He}^+$  and  $\text{Li}^+$ , using model polarization potentials for the targets. We report here calculations on six scattering systems for incident energies below the lowest inelastic threshold, as well as on 21 bound states, using a total of 35 polarization

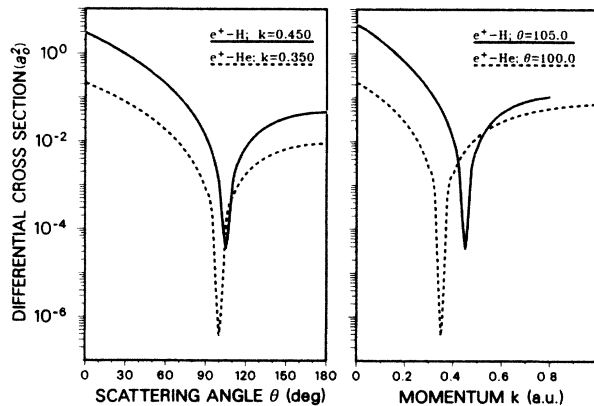


FIG. 14. Differential cross sections of positrons scattered from hydrogen and helium atoms as a function of the scattering angle at their critical energies (left) and as a function of the incident momentum at their critical angles (right).

potentials of different types. Despite the wide variety and large number of systems and polarization potential investigated, striking regularities are found among effective target radii. These give rise to universal relationships for the targets considered, and suggest the possibility that one may apply knowledge of well-known systems in accurate calculations on poorly known systems. This notion is submitted to test calculations and is found to be reliable in all cases studied.

It should be emphasized that the calculations reported here are not only accurate but also very simple. The labor required for one of our scattering or bound-state calculations with a given polarization potential is a tiny fraction of that required for an *ab initio* calculation of similar accuracy. Indeed, the numerical work required for one calculation is a small fraction of that required for several widely quoted *ab initio* calculations.

Calculations have been done on the targets neon and argon to see whether the universality of the relationships between effective target radii discovered here holds up for other targets.<sup>77</sup> Calculations are also under way in which polarization potentials are used for the lowest inelastic process, which, for all targets mentioned here, is positronium formation.

#### ACKNOWLEDGMENTS

All calculations were performed by VAX11/780, 785, and 8600 minicomputers at Marquette University Computer Services Division and all figures were generated with the aid of the ISSCO graphic package. One of us (H.N.) is grateful to the Graduate College of Marquette University and to the Author J. Schmitt Foundation for support.

<sup>1</sup>R. J. Drachman and A. Temkin, in *Case Studies in Atomic Collision in Physics II*, edited by E. W. McDaniel and M. R. C. McDowell (North-Holland, Amsterdam, 1972), p. 399.

<sup>2</sup>J. Callaway, *Comput. Phys. Commun.* **6**, 265 (1974).

<sup>3</sup>G. Peach, in *Atoms in Astrophysics*, edited by P. G. Burke, W. B. Eissner, D. G. Hummer, and I. C. Percival (Plenum, New

York, 1983), p. 1.

<sup>4</sup>J. Holtzmark, *Z. Phys.* **48**, 231 (1929); **55**, 437 (1929).

<sup>5</sup>H. S. W. Massey and A. H. A. Moussa, *Proc. Phys. Soc. London, Sect. A* **71**, 38 (1958).

<sup>6</sup>R. A. Buckingham, *Proc. R. Soc. London, Ser. A* **160**, 94 (1937); **160**, 113 (1937).

- <sup>7</sup>D. R. Bates and H. S. W. Massey, *Philos. Trans. R. Soc. London, Ser. A* **239**, 296 (1943); *Proc. R. Soc. London, Ser. A* **192**, 1 (1947).
- <sup>8</sup>M. H. Mittleman and K. M. Watson, *Phys. Rev.* **113**, 198 (1959).
- <sup>9</sup>D. M. Schrader, *Phys. Rev. A* **20**, 918 (1979).
- <sup>10</sup>H. S. W. Massey, J. Lawson, and D. G. Thompson, in *Quantum Theory of Atoms, Molecules, and Solid State*, edited by P.-O. Löwdin (Academic, New York, 1966), p. 203.
- <sup>11</sup>R. J. Drachman, *Phys. Rev.* **173**, 190 (1968); **144**, 25 (1966).
- <sup>12</sup>M. A. Morrison, T. L. Gibson, and D. Austin, *J. Phys. B* **17**, 2725 (1984).
- <sup>13</sup>R. P. McEachran and A. D. Stauffer, *J. Phys. B* **16**, 255 (1983).
- <sup>14</sup>S. K. Houston and R. J. Drachman, *Phys. Rev. A* **3**, 1335 (1971).
- <sup>15</sup>C. Schwartz, *Phys. Rev.* **124**, 1468 (1961).
- <sup>16</sup>C. L. Pekeris, *Phys. Rev.* **126**, 1470 (1962).
- <sup>17</sup>J. W. Humberston, *J. Phys. B* **6**, L305 (1973).
- <sup>18</sup>R. K. Nesbet, *J. Phys. B* **12**, L243 (1979); *Phys. Rev. A* **20**, 58 (1979).
- <sup>19</sup>C. E. Moore, *Atomic Energy Levels*, Natl. Bur. Stand. (U.S.) Circ. No. 467 (U.S. GPO, Washington, D.C., 1949).
- <sup>20</sup>S. Bashkin and J. O. Stoner, Jr., *Atomic Energy Levels and Grotrian Diagrams Vol. 1: Hydrogen I-Phosphorus XV* (North-Holland, Amsterdam, 1975).
- <sup>21</sup>E. Clementi and C. Roetti, *Atomic Data Nucl. Data Tables* **14**, 177 (1974).
- <sup>22</sup>R. Bulirsch and J. Stoer, *Numer. Math.* **8**, 1 (1966).
- <sup>23</sup>A. Dalgarno, G. W. F. Drake, and G. A. Victor, *Phys. Rev.* **176**, 194 (1968).
- <sup>24</sup>C. J. Kleinman, Y. Hahn, and L. Spruch, *Phys. Rev.* **165**, 53 (1968).
- <sup>25</sup>M. J. Seaton and L. Steenman-Clark, *J. Phys. B* **10**, 2639 (1977).
- <sup>26</sup>R. R. Treachout and R. T. Pack, *Atomic Data* **3**, 195 (1971).
- <sup>27</sup>W. R. Johnson, D. Kolb, and K.-N. Huang, *Atomic Data Nucl. Data Tables* **28**, 333 (1983).
- <sup>28</sup>M. H. Mittleman and K. M. Watson, *Ann. Phys. (N.Y.)* **10**, 268 (1960); *S. Hara, J. Phys. Soc. Jpn.* **22**, 710 (1967).
- <sup>29</sup>H. A. Bethe, *Handbuch der Physik* (Springer-Verlag, Berlin, 1933), Vol. 24/1, p. 343.
- <sup>30</sup>H. Reeh, *Z. Naturforsch.* **15a**, 377 (1960).
- <sup>31</sup>R. S. Oberoi and J. Callaway, *Phys. Rev. A* **1**, 45 (1970).
- <sup>32</sup>J. Callaway, *Phys. Rev.* **106**, 868 (1957); A. Temkin, *ibid.* **107**, 1004 (1957); **116**, 358 (1959); A. Temkin and J. C. Lamkin, *ibid.* **121**, 788 (1961).
- <sup>33</sup>K. Takayanagi and S. Geltman, *Phys. Rev.* **138**, A1003 (1965); S. Geltman and K. Takayanagi, *ibid.* **143**, 25 (1966); D. M. Schrader, *Phys. Rev. A* **20**, 933 (1979); M. Horbatsch, J. W. Darewych, and R. P. McEachran, *J. Phys. B* **16**, 4451 (1983).
- <sup>34</sup>R. I. Câmpeanu, *Z. Phys. A* **320**, 579 (1985).
- <sup>35</sup>N. F. Lane and S. Geltman, *Phys. Rev.* **160**, 53 (1967); N. F. Lane and R. J. W. Henry, *ibid.* **173**, 183 (1968); A. Dalgarno, C. Bottcher, and G. A. Victor, *Chem. Phys. Lett.* **7**, 265 (1970); P. G. Burke and N. Chandra, *J. Phys. B* **5**, 1696 (1972); M. A. Morrison, N. F. Lane, and L. A. Collins, *Phys. Rev. A* **15**, 2186 (1977); D. G. Truhler, R. E. Poling, and M. A. Brandt, *J. Chem. Phys.* **64**, 826 (1976); B. D. Buckley and P. G. Burke, *J. Phys. B* **10**, 725 (1977);  $w(\xi)=1-\exp(\xi^5)$  was used in L. Biermann, *Z. Astrophys.* **22**, 157 (1943), and  $w(\xi)=1-\exp(\xi^8)$  was used in L. Biermann, *Z. Astrophys.* **26**, 213 (1949), and in Ref. 29.
- <sup>36</sup>P. Valiron, R. Gayet, R. McCarroll, F. Masnou-Seeuws, and M. Philippe, *J. Phys. B* **12**, 53 (1979).
- <sup>37</sup>A. Jain and D. G. Thompson, *J. Phys. B* **15**, L631 (1982); **16**, 1113 (1983).
- <sup>38</sup>P. Khan, S. K. Datta, D. Bhattacharyya, and A. S. Ghosh, *Phys. Rev. A* **29**, 3129 (1984).
- <sup>39</sup>S. W. Wang, H. S. Taylor, and R. Yaris, *Chem. Phys.* **14**, 53 (1976).
- <sup>40</sup>F. A. Gianturco and D. G. Thompson, *J. Phys. B* **9**, L383 (1976); **13**, 613 (1980).
- <sup>41</sup>B. J. Laurenzi, *J. Chem. Phys.* **69**, 4838 (1978).
- <sup>42</sup>G. Csanak and H. S. Taylor, *J. Phys. B* **6**, 2055 (1973).
- <sup>43</sup>S.-W. Chiu and D. M. Schrader, *Phys. Rev. A* **33**, 2339 (1986).
- <sup>44</sup>R. Armstead, *Phys. Rev.* **171**, 91 (1968).
- <sup>45</sup>D. Register and R. T. Poe, *Phys. Lett.* **51A**, 431 (1975).
- <sup>46</sup>J. F. Williams, *J. Phys. B* **12**, 265 (1979).
- <sup>47</sup>A. K. Bhatia, A. Temkin, R. J. Drachman, and H. Eiserike, *Phys. Rev. A* **3**, 1328 (1971); M. A. Abdel-Raouf and D. Belschner, *J. Phys. B* **11**, 3677 (1978).
- <sup>48</sup>A. K. Bhatia, R. J. Drachman, and A. Temkin, *Phys. Rev. A* **9**, 223 (1974).
- <sup>49</sup>J. W. Humberston and R. J. Câmpeanu, *J. Phys. B* **13**, 4907 (1980).
- <sup>50</sup>R. I. Câmpeanu, Ph.D. thesis, University of London, 1977.
- <sup>51</sup>A. S. Ghosh, N. C. Sil, and P. Mandal, *Phys. Rep.* **87**, 313 (1982).
- <sup>52</sup>J. K. O'Connell and N. F. Lane, *Phys. Rev. A* **27**, 1893 (1983).
- <sup>53</sup>J. C. Nickel, K. Imre, D. F. Register, and S. Trajmar, *J. Phys. B* **18**, 125 (1985).
- <sup>54</sup>W. R. Newell, D. F. Brewer, and A. C. H. Smith, *J. Phys. B* **14**, 3209 (1981).
- <sup>55</sup>M. Charlton, T. C. Griffith, C. R. Heyland, and T. R. Twomey, *J. Phys. B* **13**, L239 (1980).
- <sup>56</sup>G. Sinapius, W. Raith, and W. G. Nilson, *J. Phys. B* **13**, 4079 (1980).
- <sup>57</sup>D. R. Register, S. Trajmar, and S. K. Srivastava, *Phys. Rev. A* **21**, 1134 (1980).
- <sup>58</sup>H. B. Milloy and R. W. Crompton, *Phys. Rev. A* **15**, 1847 (1977).
- <sup>59</sup>R. W. Crompton, M. T. Elford, and A. G. Robertson, *Aust. J. Phys.* **23**, 667 (1970).
- <sup>60</sup>J. R. Winick and W. P. Reinhardt, *Phys. Rev. A* **18**, 910 (1978).
- <sup>61</sup>Y. F. Chan and R. A. Fraser, *J. Phys. B* **6**, 2504 (1973).
- <sup>62</sup>Y. F. Chan and R. P. McEachran, *J. Phys. B* **9**, 2869 (1976).
- <sup>63</sup>R. P. McEachran and P. A. Fraser, *Proc. Phys. Soc. London* **86**, 369 (1965).
- <sup>64</sup>R. J. Drachman, *Phys. Rev.* **138**, A1582 (1965).
- <sup>65</sup>R. I. Câmpeanu and J. W. Humberston, *J. Phys. B* **8**, L244 (1975); **10**, L153 (1977).
- <sup>66</sup>R. P. McEachran, D. L. Morgan, A. G. Ryman, and A. D. Stauffer, *J. Phys. B* **10**, 663 (1977); R. P. McEachran, D. L. Morgan, A. G. Ryman, and A. D. Stauffer, *ibid.* **11**, 951 (1978).
- <sup>67</sup>M. Ya Amusia, N. A. Cherepkov, L. V. Chernysheva, and S. G. Shapiro, *J. Phys. B* **9**, L531 (1976).
- <sup>68</sup>T. Mizogawa, Y. Nakayama, T. Kawaratani, and M. Tosaki, *Phys. Rev. A* **31**, 2171 (1985).
- <sup>69</sup>P. G. Coleman, J. D. McNutt, L. M. Diana, and J. R. Burciaga, *Phys. Rev. A* **20**, 145 (1979).
- <sup>70</sup>T. S. Stein, W. E. Kauppila, V. Pol, J. H. Smart, and G. Jesion, *Phys. Rev. A* **17**, 1600 (1978).
- <sup>71</sup>K. F. Canter, P. G. Coleman, T. C. Griffith, and R. G. Heyland, *J. Phys. B* **5**, L167 (1972); **6**, L201 (1973).
- <sup>72</sup>J. F. Williams, *J. Phys. B* **8**, 1683 (1975).
- <sup>73</sup>T. F. O'Malley, J. Rosenberg, and L. Spruch, *Phys. Rev.* **125**,

- 1300 (1962).
- <sup>74</sup>D. G. Thompson, Proc. R. Soc. London, Ser. A **294**, 160 (1966).
- <sup>75</sup>J. M. Wadehra, T. S. Stein, and W. E. Kauppila, Phys. Rev. A **29**, 2912 (1984).
- <sup>76</sup>R. P. McEachran, A. G. Ryman, and A. D. Stauffer, J. Phys. B **12**, 1031 (1979); R. P. McEachran, A. D. Stauffer, and L. E. M. Campbell, *ibid.* **13**, 1281 (1980).
- <sup>77</sup>H. Nakanishi and D. M. Schrader, following paper, Phys. Rev. A **34**, 1823 (1986).

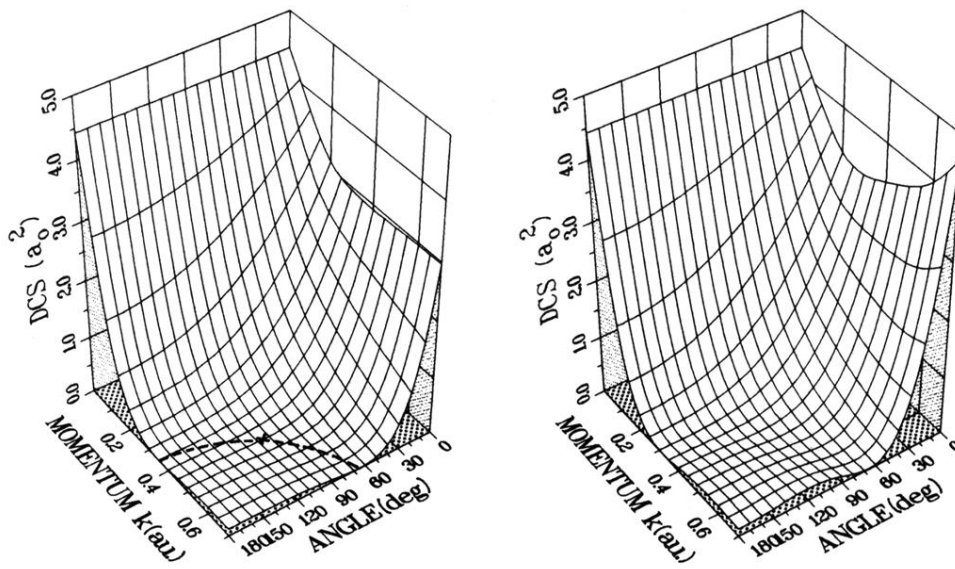


FIG. 12. Differential cross sections (DCS's) of a positron elastically scattered from a hydrogen atom (left, present work; right, best values). The cutoff function with  $m=2$  and  $n=8$  and  $r_0^+=1.926$  is used. The dashed curve and the  $\times$  represent the locus of the differential cross-section minima and the critical point. Best values are calculated from  $s$ -,  $p$ -, and  $d$ -wave phase shifts from Refs. 47, 48, and 45, respectively.

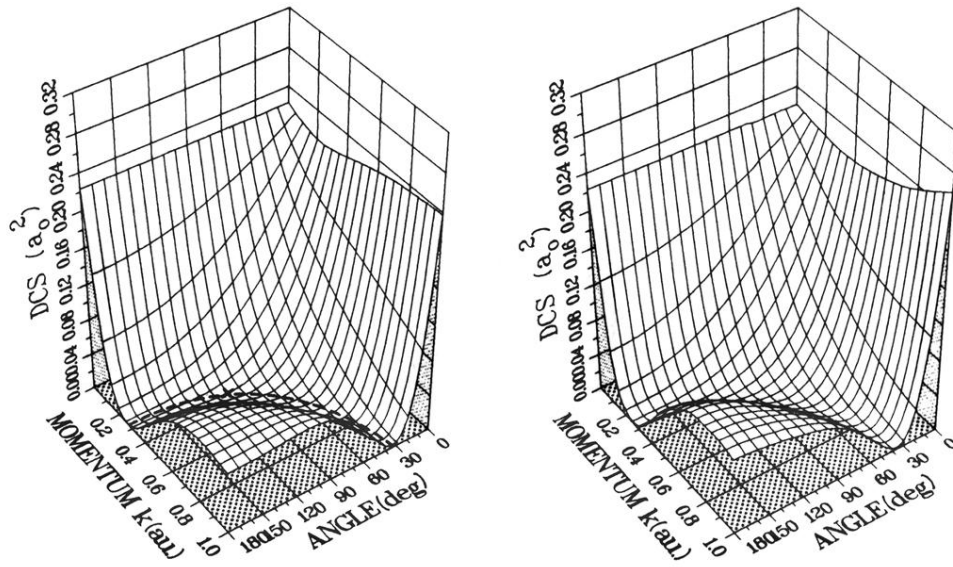


FIG. 13. Differential cross sections of a positron elastically scattered from a helium atom (left, present work; right, best values). The cutoff function with  $m = 2$  and  $n = 8$  and  $r_0^+ = 1.424$  is used. The dashed curve and the  $\times$  represent the locus of the differential cross-section minima and the critical point. Best values are calculated from  $s$ -,  $p$ -, and  $d$ -wave phase shifts from Refs. 17, 49, and 50, respectively.